INVESTIGATIONS OF INJECTION ORBITS AT CESR BASED ON TURN-BY-TURN BPM MEASUREMENTS*

M. G. Billing†, J. A. Crittenden, M. A. Palmer, LEPP, Cornell University, Ithaca, NY 14850, USA

Abstract

A data acquisition system permitting turn-by-turn orbit measurements has been employed at CESR to study the optics for the injected electron beam. An optimization algorithm uses these measurements to determine the effective lattice functions describing the behavior of the injected electrons. We present the application of these measurements to calculations of injection acceptance envelopes, which include parasitic beam-beam interactions with the stored positron beam.

INJECTION INTO CESR

Injection into the Cornell Electron Storage Ring (CESR) uses a full betatron wavelength bump at the injection point with a half-sinewave amplitude lasting 4 rotation periods (turns.) At its peak, this closed bump places the stored beam's centroid within 4 horizontal sigma of the vacuum chamber wall and leaves the injected beam to oscillate with an amplitude equal to the displacement between injected and stored beams. A pinger magnet applies a constant deflection to the beam for one turn, increasing the stored beam's amplitude while decreasing the injected beam's oscillation amplitude.

With the introduction of horizontal pretzel separation for multi-bunch beams in CESR, the aperture available in the arcs for electron injection was reduced by what is needed for the positron beam. Several techniques were developed to improve injection under these conditions. The first operated with different tunes for the two beams to reduce the parasitic beam-beam coupling effects by controls using the differential horizontal displacements of the beams in the sextupoles. Another was to inject electrons on the coupling resonance, effectively reducing the emittance of the horizontal eigenmode at the expense of the vertical. Because of the large coherent tune shift from the beam-beam interaction during electron filling, the coupling resonance width needed be large enough to maintain the electron beam on resonance. Also, off-energy injection is routinely employed to reduce the betatron motion of the injected electrons at the expense of increasing the synchrotron motion. Lastly, bunch-by-bunch beam stabilizing feedback was added to damp coherent horizontal, longitudinal and vertical motion. The greatest demand is placed on the aperture during the injection of electrons in the presence of the stored positron beam, since this requires adequate apertures for the injected bunches of electrons and both stored beams.

During the last few years CESR has been operating for HEP near the charm threshold (1.5 to 2.5 GeV) with the addition of 12 superconducting wigglers or at energies of 5 GeV for synchrotron light. At low energy, the injection repetition rate must be reduced from 60 Hz to 30 Hz to permit enough damping of the injected electrons before the next injection cycle. Also at low energy the multiple scattering of the injected beam in the thin window separating the vacuum of the transport line from CESR's vacuum causes an increase in the angular distribution by about a factor of 3. Some new tools (described below) have been developed to assist in the study of injection and in certifying the quality of new optics designs.

* Work supported by the National Science Foundation.
† mgb@cesr10.lepp.cornell.edu

ANALYSIS OF INJECTION TRANSIENTS

In 2002 the electronics for 15 (of the 100 total) beam position monitors (BPM's) in CESR were upgraded to give higher position resolution and the acquisition of 1000 turns of position and intensity data for stored or injected beam currents, allowing the collection of BPM data in a variety of injection conditions[1]. Software was developed for analyzing these transient measurements by projecting freely propagating uncoupled betatron and energy oscillations forward from the injection point in CESR. The analysis begins by subtracting the average horizontal and vertical position from the data. The remaining "transient" is fit for the parameters a_0, a_1, c_0, and c_1 in the following general form, using all the BPM's beginning on the n_0–th turn for then next N turns,

$$\chi^2 = \sum_d \sum_{n=n_0}^{n_0+N} \left\{ x_{dn} - \langle x_{dn} \rangle - \begin{pmatrix} 1 & 0 \end{pmatrix} T_{d0} \, T_{00}^m \begin{pmatrix} a_0(n_0) \\ a_1(n_0) \end{pmatrix} - \begin{pmatrix} \eta_d & 0 \end{pmatrix} \begin{pmatrix} \cos m\mu_z & \sin m\mu_z \\ -\sin m\mu_z & \cos m\mu_z \end{pmatrix} \begin{pmatrix} c_0(n_0) \\ c_1(n_0) \end{pmatrix} \right\}^2$$

with $m = n - n_0$, d the detector index, x_{dn} the position at detector d on the n-th turn and the angle brackets denote the average. In this equation, T_{00} is the 2-by-2 one turn betatron transport matrix at the injection point, T_{d0} is the transport matrix from the injection point to detector d. The dispersion at d is denoted as η_d and the phase advance is $\mu_z = 2\pi Q_z$, with Q_z denoting the synchrotron tune. The fourth term in the fit represents the single-turn transport of the synchrotron oscillation and is appropriate since the 15 detectors occupy a short contiguous region of the ring. The equation for χ^2 above is used in this form for the analysis of the horizontal BPM data; the second term is excluded when fitting the vertical BPM data. In addition, the matrix T_{00} is written explicitly in terms of $\mu_{x,y} = 2\pi Q_{x,y}$ where Q_x and Q_y are the betatron tunes. The tunes are then varied to minimize the fit and, using these tunes, a_0, a_1, c_0, and c_1 are again calculated; this process is iterated to give a minimum χ^2.

For CESR, N is chosen to be 42 turns to encompass about 4 synchrotron oscillation periods. The fit begins on

turn 5 to be certain that the bumper and pinger magnets have finished pulsing; this allows the beam's motion to propagate as free betatron and synchrotron oscillations. The results are presented as the projection of the initial injection coordinates, x, x', y, y', δ, and δ' = Δz / (α_p C), where Δz is the change of path length, α_p is the momentum compaction factor and C is the circumference of the ring. These results are also written in terms of action-angle variables, A_x, θ_x, A_y, θ_y, A_z, and θ_z. In addition, the fitted values of μ_x, μ_y, and μ_z are displayed. A set of 9 plots gives the projected initial injection coordinates in action-angle variables and the three oscillation phase advances per turn as a function of the starting turn as n_0 is moved along in 7 turn steps. To account for systematic tune changes within the data, the projected injection angles are corrected with the fitted values of μ_x, μ_y, and μ_z coming from windows starting at earlier turns. The successful correction of the tunes is visible as constant projected θ_x, θ_y, or θ_z as n_0 is varied.

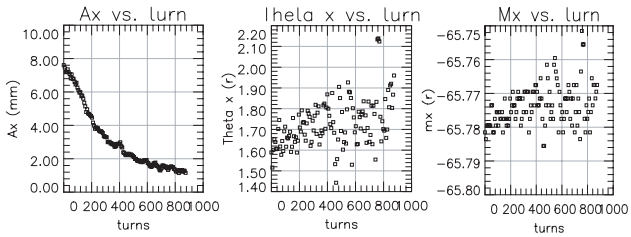

Figure 1. Plots of A_x and θ_x vs. the initial turn number of the 42 turn fit window as the initial turn is changed. In the remaining plot, M_x refers to μ_x.

Case	Amplitude		
	Horizontal	Vertical	Longitudinal
A	7.4 ± 0.7 mm	1.3 ± 0.1 mm	4.7 ± 0.2 x 10^{-3}
B	1.6 ± 0.3 mm	0.17 ± 0.02 mm	0.1 ± 0.1 x 10^{-3}
C	3.5 ± 0.3 mm	0.39 ± 0.05 mm	0.2 ± 0.1 x 10^{-3}

Table 1. Transient position measurements at 1.8 GeV for injection conditions with different pulsed elements firing: A) Injected electrons with pulsed bump and pinger magnets, B) Stored electrons with pulsed bump magnets and C) Stored electrons with pinger magnet only. The horizontal and vertical results are the oscillation amplitudes, while the longitudinal is the fractional energy deviation amplitude.

As an example, Figure 1 shows the plots of the horizontal fits as n_0 is varied. The fits yield an initial 7.6 mm oscillation amplitude, which "damps" in about 400 turns, while over the same time, μ_x remains relatively constant (as seen in the relatively flat fits for both μ_x and θ_x.) This "damping" of the motion is not due to radiation damping, which is approximately 34,000 turns, or feedback (as the injected bunch signal is below the system's noise threshold), but rather represents the decoherence of the bunch's motion. When the position signal decoheres sufficiently after turn 420, the fit of μ_x and θ_x becomes poor.

During January 2003 at 1.8 GeV, sets of trajectories for the injected or stored beams undergoing injection transients were acquired under different conditions and analyzed. A summary of these results is in Table 1; the uncertainties represent a combination of statistical and estimated systematic errors. All results are projections to the injection point at the injection time of the electrons. The total displacement of the injected beam relative to the stored beam at the septum magnet equals the sum of the amplitude for the injected beam from the pulsed bump, the amplitude for the stored beam from the pinger and the dispersion at the injection point (1.5 m) times the fractional energy error, giving 18 mm in reasonably good agreement with what was expected.

CHARACTERIZING OPTICS DESIGNS

The ability to measure the injection trajectories with reasonable accuracy suggests that this may be applied to improve the modeling of electron injection against stored positrons, leading to a more realistic computation of the physical space required by the injected and stored beams during the injection process. The physical space required for each beam is defined as the volume that contains the injection oscillations plus some number of sigma for the beam's size. An alternate method to tracking multiple particles (representing the distribution of the beams and determining the survivors) has been created as a much less computationally intensive approach to studying the injection properties of a set of optics.

The new approach defines an envelope for each beam as the physical space occupied by the beam's centroid; the method is most useful when the motion of the centroid is larger than the transverse size of the injected beam. Defining the beam's envelope simplifies the need to determine the particle distribution in the bunch immediately preceding injection. This method assumes that, as a beam undergoes betatron or synchrotron oscillations, any damping of this motion occurs after a large number of oscillation periods so that the maximum amplitude of the oscillation is achieved at every point around the storage ring. This additional assumption gives a limiting envelope for the beam at each element in the storage ring. The present calculation includes the parasitic crossings of the beam, which modify the beta functions and the pretzel orbit for the central particles as a function of the positron beam current. From the envelope and the known pretzel orbits of each beam, the clearance of the envelope from either the physical aperture or the center of the other beam is then computed. The analysis software presents this clearance both in the units of length and in terms of the number sigma of stored beam.

The envelope equations, which detail the injection process into CESR, are described elsewhere[2]. The results may be summarized (for simplicity in only the x-direction) as follows. At each position, s, in the ring the local beta-function β_x and dispersion η_x, the pretzel

displacement of the orbit for the stored beam x_p and maximum displacement due to the pulsed bump x_{PB} are required. All betatron injection oscillations are characterized by their equivalent action (same units as the emittance), and energy oscillations by their maximum fractional energy amplitude, and these were determined from the measurements, described in the previous section.

Thus the wall clearance for the stored electrons $x_{c,\ se}$ is

$$x_{c,se} = A_{wall} - |x_P| - \max\left\{|x_{PB}|,\ \left|\sqrt{A_{se}\ \beta_x}\right|\right\} - |\eta_x\ \ \delta_{w,se}|$$

where A_{se} is the horizontal action from residual betatron oscillations and $\delta_{w,se}$ is the energy oscillation amplitude. Both are produced for the stored electrons by the pinger and any non-closure of the pulsed bumps, causing the half aperture A_{wall} to be reduced by the displacement of the pretzeled orbit and the stored electron envelope. Negative values imply the center of the beam touches the wall. The action of the betatron injection oscillation A_{ie} is

$$\beta_{x,I} A_{ie} = x_I - |x_{P,I}| - |\eta_{x,I}\ \ \delta_{ie}| - \sqrt{A_{Ping,ie}\beta_{x,I}} - |x_{PB,I}|$$

where the subscript I designates the value is taken at the injection point, x_I is the displacement of the injected beam from the storage ring axis, δ_{ie} is the fractional energy error of the injected beam and $A_{Ping,\ ie}$ is the action removed from the injected beam's oscillation by the pinger magnet. Thus the injected beam's wall clearance may be written as

$$x_{c,ie} = A_{wall} - |x_p| - \sqrt{A_{ie}\ \ \beta_x} - |\eta_x\ \ \delta_{ie}|$$

and the injected beam's clearance of the center of the stored positrons $x_{c,ie+}$ is

$$x_{c,ie+} = 2\ |x_p| - x_{ie} - \sqrt{A_{se}\ \ \beta_x} - |\eta_x\ \ \delta_{se}|$$

where the last two terms give the positron beam's envelope. This expression assumes that the pretzel displacement is opposite in sign for the stored positron beam and the magnitudes of the oscillation transients are same for the stored positron and electron beams.

Figure 2 shows the wall clearances for the stored and injected electron beams in the present 1.8 GeV optics. The wall clearance for the stored beam is at least 21 mm in the arcs of CESR, except in the region of the pulsed bump (plotted in blue.) The stored beam is permitted a much closer approach to the injection septum, since the pulsed bump only places the stored beam close to the wall for one turn per injection cycle. The wall clearance is at least 9 horizontal sigma around the ring except in the pulsed bump. Notice the pulsed bump clearance at 510 m (the injection point) is greater than at 520 and 560 m. This set of optics requires closed orbit bumps placed with peaks near 520 and 560 m to improve the lifetime of the stored beam when the pulsed bump is triggered.

Figure 3 shows the clearance of the injected electrons from the stored positron beam. Here the results show that, although the injected beam clears the center of the stored positron beam most places in the arcs, it will approach the center of the positron beam in two locations. There has been generally good agreement between the predicted injection properties of optics using this method and the actual injection performance.

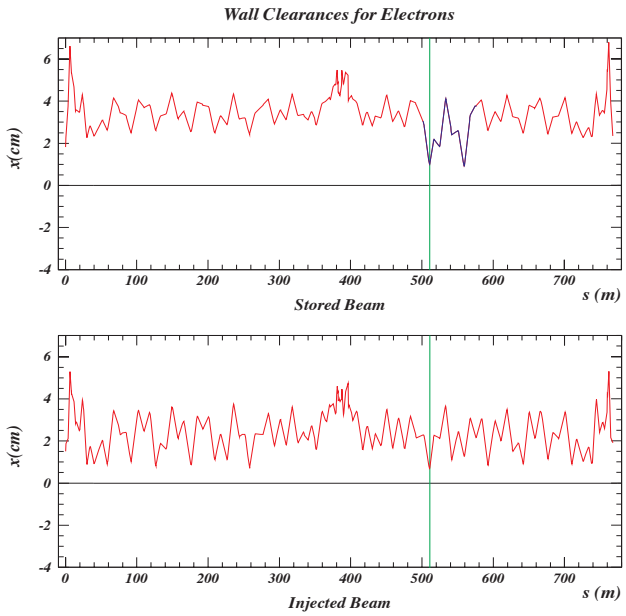

Figure 2. Computed wall clearances for the stored and injected electron beams around the entire storage ring. The blue section of the stored electron wall clearance plot represents the reduced clearance on one turn due to the pulsed bump. The green line marks the injection point.

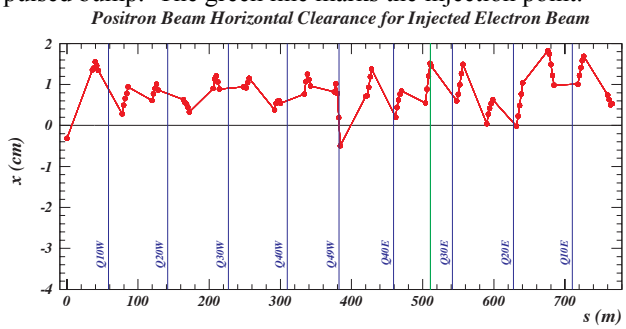

Figure 3. Clearance between the stored positron beam and the injected electrons. The dots in the plot indicate the parasitic crossings where the injected electrons encounter trains of positrons bunches. The crossings near 384 m also are separated vertically.

CONCLUSIONS

The analysis of BPM data, taken during injection transients, yields valuable input for a new method of evaluating injection optics based on the envelopes of the injection oscillations and the clearance of the beam centroids from the aperture and the counter-rotating beam.

REFERENCES

[1] M. Palmer et al, "An Upgrade for the Beam Position Monitoring System at the Cornell Electron Storage Ring", Proc. of the 2001 IEEE Part. Accel. Conf, p. 1360.

[2] M. G. Billing, et al, "Recent Developments for Injection into CESR", ICFA Beam Dynamics Newsletter, No. 31, Aug. 2003, p.58, http://icfa-usa.jlab.org/archive/newsletter/icfa_bd_nl_31.pdf